Int J Clin Exp Pathol 2016;9(8):7908-7918
www.ijcep.com /ISSN:1936-2625/IJCEP0025885

Original Article

Snail-induced CD44^{high} cells in HNSCC with high ABC transporter capacity exhibit potent resistance to cisplatin and docetaxel

Miho Hashikata[1], Hideo Shigeishi[1], Gaku Okui[1], Kazuhiro Yamamoto[1], Kei Tobiume[1], Sayaka Seino[1], Ryo Uetsuki[1], Hiroki Kato[1], Yasuki Ishioka[1], Shigehiro Ono[1], Kouji Ohta[1], Koichiro Higashikawa[1], Masaru Sugiyama[2], Masaaki Takechi[1]

Departments of [1]Oral and Maxillofacial Surgery, [2]Public Oral Health, Institute of Biomedical and Health Sciences, Hiroshima University, 1-2-3 Kasumi, Minami-ku, Hiroshima 734-8553, Japan

Received February 12, 2016; Accepted June 11, 2016; Epub August 1, 2016; Published August 15, 2016

Abstract: CD44^{high} head and neck squamous cell carcinoma (HNSCC) cells with cancer stem cell (CSC)-like properties have been speculated to be involved in resistance to apoptosis induced by anti-cancer drugs and thereby associated with tumor recurrence. To clarify the chemotherapeutic resistance of CD44^{high} HNSCC cells, we examined the apoptotic effects of cisplatin and docetaxel in sorted populations (i.e., CD44^{high}/ESA^{low}, CD44^{high}/ESA^{high} and CD44^{low} cells) from the HNSCC cell line HTB-41. Furthermore, we examined whether Snail, which leads to the epithelial to mesenchymal transition (EMT) program, can induce formation of CD44^{high}/ESA^{low} cells in an HNSCC cell population. CD44^{high}/ESA^{low} cells showed mesenchymal features and potent resistance to both cisplatin- and docetaxel-induced apoptosis. siRNA knockdown of ABCC2 significantly induced apoptosis of CD44^{high}/ESA^{low} cells in the presence of cisplatin, while ABCG2 knockdown induced apoptosis of those cells in the presence of docetaxel. These findings suggest that strong resistance to cisplatin by CD44^{high}/ESA^{low} cells may be attributable to a high level of ABC transporter activity. Furthermore, development of CD44^{high}/ESA^{low} cells was induced in the HNSCC cell line OM-1 by Snail transfection and those sorted from OM-1 cells harboring a Snail-transgene showed strong resistance to cisplatin- and docetaxel-induced apoptosis. Our results indicate that CD44^{high}/ESA^{low} HNSCC cells play important roles in cisplatin and docetaxel resistance caused by high drug efflux activity. Furthermore, Snail may be involved in induction of both mesenchymal characteristics and CSC-like properties of HNSCC cells. A better understanding of the phenotypic plasticity of HNSCC cells is necessary to improve the results of chemotherapy with cisplatin and docetaxel.

Keywords: Head and neck squamous cell carcinoma (HNSCC), CD44, snail, apoptosis, epithelial to mesenchymal transition (EMT)

Introduction

Head and neck squamous cell carcinoma (HNSCC) is the sixth most prevalent cancer worldwide with high morbidity, with approximately 500,000 new cases diagnosed each year [1, 2]. Despite recent advances in treatment options including combinations of surgery, radiation, and chemotherapy, the survival rates of affected patients have not been sufficiently improved [3-5]. Mortality is mainly related to local recurrence and metastasis. Furthermore, since most chemotherapeutic agents lack selective cancer efficacy, resistance to those drugs is commonly observed. It is vital to elucidate the molecular mechanisms that contribute to drug resistance in order to improve therapeutic approaches for treating patients with head and neck cancer.

Tumor recurrence and metastasis are thought to be associated with a small population of cancer cells with stem cell-like properties (i.e., cancer stem cells; CSCs) in HNSCC [6]. CSCs have been speculated to be involved in resistance to apoptosis induced by anti-cancer drugs and thereby related to tumor recurrence [7], thus it is necessary to clarify the mechanisms of therapeutic resistance in these cells. CD44 was previously identified as a significant marker of

CSCs in HNSCC [8]. Using FACS analysis of the expressions of CD44 and epithelial specific antigen (ESA), HNSCC cells with an elevated expression of CD44 and mesenchymal characteristics (i.e., CD44^{high}/ESA^{low} cells) were sorted and shown to have CSC properties, such as high clonogenic ability and tumor forming ability [9]. In addition, CD44^{high}/ESA^{low} cells exhibited high resistance to 5-FU-induced apoptosis along with a high level of DPD expression [10]. These results indicate the possibility that CD44^{high}/ESA^{low} cells may be involved in high resistance to other chemotherapeutics in patients with HNSCC. In the present study, we investigated the sensitivity to platinum and docetaxel, as well as the expression of drug efflux transporters, known as ATP-binding cassette (ABC) transporters, in sorted HNSCC cells (CD44^{high}/ESA^{low}, CD44^{high}/ESA^{high}, CD44^{low}). Furthermore, we examined whether Snail, which leads to the epithelial to mesenchymal transition (EMT) program, can induce the development of CD44^{high} cells with high resistance to chemotherapeutics used to treat HNSCC.

Materials and methods

Cell cultures and fluorescence-activated cell sorting

The human HNSCC cell line HTB-41 was obtained from American Type Culture Collection (ATCC) (Manassas, VA, USA). HTB-41 and the HNSCC cell line OM-1 [11] were cultivated in Dulbecco's Modified Eagle's Medium (DMEM) with 10% FBS under 5% CO_2 in air at 37°C. For re-plating and assays, cells were released into the suspension using Accutase (Innovative Cell Technologies, San Diego, CA). To examine the effect of PGE_2, cells were exposed to medium without FBS for 48 hours. PGE_2 (Sigma-Aldrich, St. Louis, MO) was added at a final concentration of 10 μg/ml. SC-51089 (Enzo Life Science, PA) was used as an EP1 receptor inhibitor at a final concentration of 100 μg/ml and AH-6809 (Cayman Chemical, Michigan, USA) as an EP1/EP2 receptor inhibitor at a final concentration of 100 μg/ml.

Fluorescence-activated cell sorting

FACS analyses using an anti-CD44-PE-conjugated antibody and anti-ESA-APC-conjugated antibody, both from BD Biosciences (Tokyo, Japan) were performed, with 7-AAD (BD Biosciences) used to exclude dead cells. Samples were assayed using a Becton Dickenson FACSCalibur™ (BD Biosciences). Cells with a high expression of CD44 and low expression of ESA (CD44^{high}/ESA^{low}), those with a high expression of both markers (CD44^{high}/ESA^{high}), and those with low a level of CD44 expression (CD44^{low}) were sorted using a Becton Dickenson FACSAria device. The obtained data were analyzed using FACS Diva version 6.1.1 software (BD Biosciences).

Apoptosis analyses

Cisplatin (Wako, Osaka, Japan) and docetaxel (LKT Laboratories, St. Paul, MN) were used to induce apoptosis in FACS-sorted populations of HNSCC cells. Cells at 5.0×10^4 were seeded into 6-well plates, then after 24 hours were exposed to 5 μg/ml cisplatin or 1 μg/ml docetaxel for 48 hours. Cells were collected and stained with 7-AAD and Annexin V-Cy5 (BD Pharmingen, San Diego, CA) before FACS analysis to identify AnnexinV-positive apoptotic fractions. The results are expressed as the mean ± SD for 3 independent experiments.

Side population analysis

Cells (1.0×10^6 cells/ml) were labeled with 2.0 μg/ml Hoechst 33342 (Sigma-Aldrich) for 90 minutes at 37°C. The control cells were incubated in the presence of 30 μg/ml verapamil (Sigma-Aldrich). Analysis of the side population was performed using FACSAria II (BD Biosciences). Dead cells were identified on the basis of 7-AAD (BD Pharmingen) staining and excluded.

RNA extraction and quantitative RT-PCR analysis

RNA was extracted using an RNAeasy micro kit (Qiagen, Hilden, Germany), and then 1 μg of total RNA was subjected to RT using a High Efficient Reverse Transcription Kit (TOYOBO, Osaka, Japan). Quantification of mRNA levels was performed using a CFX connect real-time PCR detection system (BioRad, Hercules, CA) and SYBR Green PCR Master Mix (TOYOBO). The reaction mixture contained 1.0 μg cDNA, 12.5 μl SYBR Green Mix, and 10 μmol of each pair of oligonucleotide primers. GAPDH was used as the reference mRNA control. The PCR program was performed as follows: initial melt-

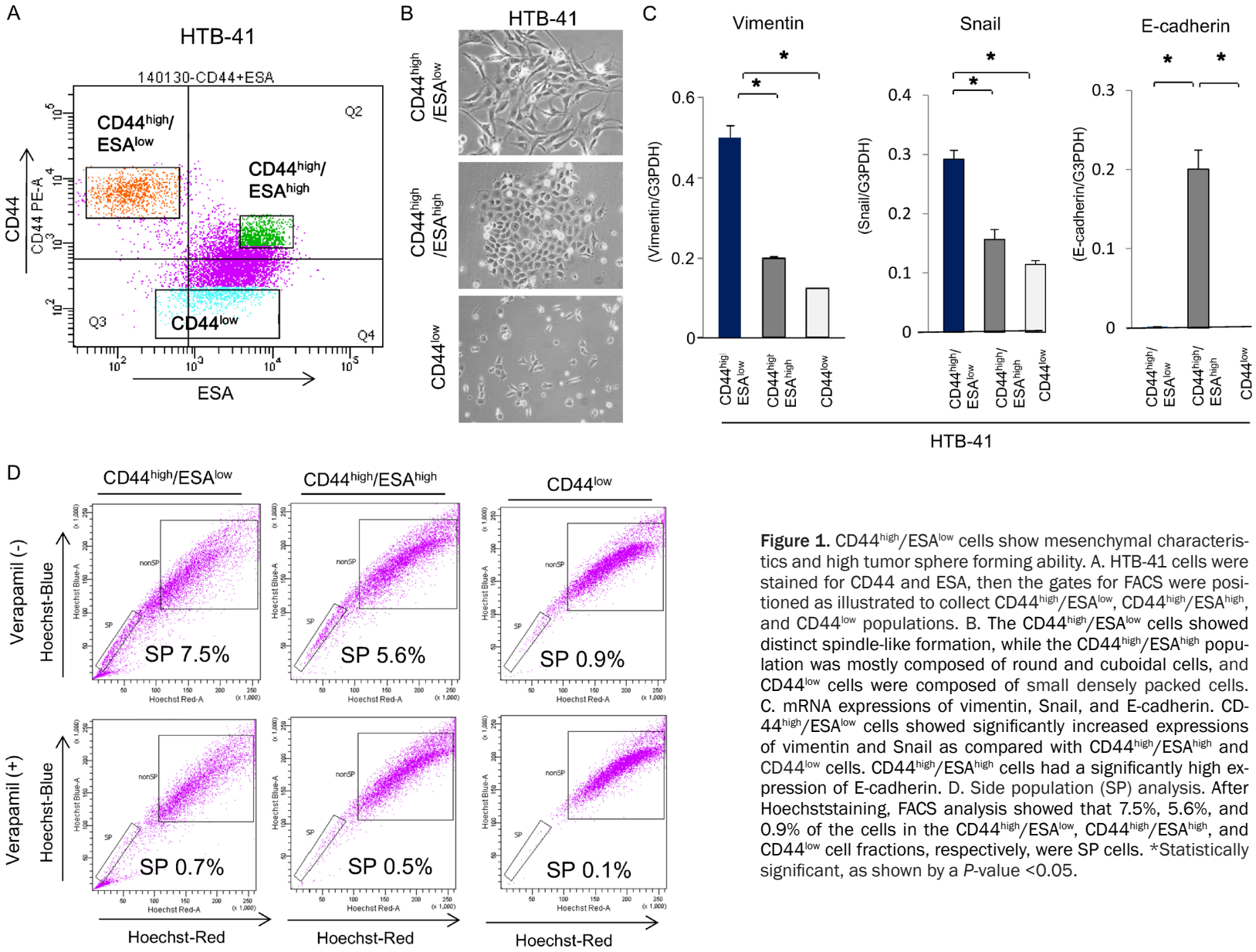

Figure 1. CD44^{high}/ESA^{low} cells show mesenchymal characteristics and high tumor sphere forming ability. A. HTB-41 cells were stained for CD44 and ESA, then the gates for FACS were positioned as illustrated to collect CD44^{high}/ESA^{low}, CD44^{high}/ESA^{high}, and CD44^{low} populations. B. The CD44^{high}/ESA^{low} cells showed distinct spindle-like formation, while the CD44^{high}/ESA^{high} population was mostly composed of round and cuboidal cells, and CD44^{low} cells were composed of small densely packed cells. C. mRNA expressions of vimentin, Snail, and E-cadherin. CD44^{high}/ESA^{low} cells showed significantly increased expressions of vimentin and Snail as compared with CD44^{high}/ESA^{high} and CD44^{low} cells. CD44^{high}/ESA^{high} cells had a significantly high expression of E-cadherin. D. Side population (SP) analysis. After Hoechststaining, FACS analysis showed that 7.5%, 5.6%, and 0.9% of the cells in the CD44^{high}/ESA^{low}, CD44^{high}/ESA^{high}, and CD44^{low} cell fractions, respectively, were SP cells. *Statistically significant, as shown by a *P*-value <0.05.

ing at 95°C for 10 minutes, followed by 40 cycles at 95°C for 15 seconds, 60°C for 30 seconds, and 72°C for 40 seconds. Results are expressed as the mean ± SD for 3 independent experiments. Semi-quantitative RT-PCR was performed with 28 cycles of denaturing at 95°C for 30 seconds, then annealing at 57°C for 30 seconds and extension at 72°C for 60 seconds. The PCR products were separated by electrophoresis on 2% agarose gels and visualized by staining with ethidium bromide. The primer sequences were as follows: vimentin; 5'-CCCTCACCTGTGAAGTGGAT-3' (sense) and 5'-GACGAGCCATTTCCTCCTTC-3' (antisense), E-cadherin; 5'-GAACGCATTGCCACATACAC-3' (sense) and 5'-AGCACCTTCCATGACAGACC-3' (antisense), Snail; 5'-CAAGGAATACCTCAGCCTGG-3' (sense) and 5'-CATCTGAGTGGGTCTGGAGG-3' (antisense), ABCC2; 5'-TGAGCAAGTTTGAAACGCACAT-3' (sense) and 5'-AGCTCTTCTCCTGCCGTCTCT-3' (antisense), ABCG2; 5'-GCTGCAAGGAAAGATCCAAG-3' (sense) and 5'-TCCAGACACACCACGGATAA-3' (antisense), CD44; 5'-TCCAACACCTCCCAGTATGACA-3' (sense) and 5'-GGCAGGTCTGTGACTGATGTACA-3' (antisense), ESA; 5'-CAATGCAGGGTCTAAAAGCTG-3' (sense) and 5'-CACCCATCTCCTTTATCTCAGC-3' (antisense), and G3PDH; 5'-GTGAACCATGAGAAGTATGACAAC-3' (sense) and 5'-ATGAGTCCTTCCACGATACC-3' (antisense).

Introduction of Snail through viral infection

Using our previously reported method, we prepared a pool of OM-1 cells harboring the Snail transgene (OM-1 Snail pool) using a retrovirus vector [12]. Briefly, Snail (GenBank accession number: AF155233) ORF cDNA was amplified from an OM-1 cDNA library using LA Taq with a GC Buffer kit (TakaraBio, Shiga, Japan). Virus host cells (HEK293FT cells) were co-transfected with a viral vector plasmid (pBabe-puro; Cosmo Bio, Tokyo, Japan) and packaging plasmid (pVSV-G; Invitrogen) using FuGENE6 (Roche, Basel, Switzerland). After 48 hours, the viral supernatant was used to infect the OM-1 cells.

Statistical methods

Statistical analysis was performed using Student's t-test or one-way analysis of variance (ANOVA). At least 3 independent samples were used for each experiment. *P* values less than 0.05 were regarded as statistically significant.

Results

CD44^{high} HNSCC cells showed both epithelial and mesenchymal phenotypes

Cells from the HNSCC cell line HTB-41 were fractionated by fluorescence-activated cell sorting (FACS) to isolate CD44^{high}/ESA^{low}, CD44^{high}/ESA^{high}, and CD44^{low} cells from gates positioned as shown in **Figure 1A**. Among these HTB-41 cells, CD44^{high}/ESA^{low} cells showed distinct spindle formation (**Figure 1B**), and high expression levels of vimentin and Snail (**Figure 1C**). Furthermore, CD44^{high}/ESA^{high} cells exhibited round and cuboidal formations, and a high expression of E-cadherin (**Figure 1B**, **1C**), while CD44^{low} cells were composed of small and densely packed cells (**Figure 1B**). Cell fractions with high ABC transporter activity were observed as a side population (SP) by Hoechst 33342 dye staining. Using FACS analysis, the percentage of SP cells among the CD44^{high}/ESA^{low}, CD44^{high}/ESA^{high}, and CD44^{low} cell fractions was found to be 7.5%, 5.6%, and 0.9%, respectively (**Figure 1D**). In addition, cells with high ABC transporter activity were found in the CD44^{high}/ESA^{low} and CD44^{high}/ESA^{high} populations, while the CD44^{low} group showed a very low percentage of SP cells (**Figure 1D**).

CD44^{high}/ESA^{low} cells exhibited strong apoptotic resistance to cisplatin and docetaxel with high expression of the ABC transporter gene

To clarify chemotherapeutic resistance in each sorted population, we examined the apoptotic effects of cisplatin and docetaxel using FACS analysis of cells stained with Annexin V-Cy5. Significant differences in the percentages of apoptotic cells were found among the groups, with apoptotic cells shown to comprise 9.2±1.9%, 13.0±0.77%, and 26.8±0.54% of the CD44^{high}/ESA^{low}, CD44^{high}/ESA^{high}, and CD44^{low} fractions of HTB-41 cells, respectively (**Figure 2A**). Thus CD44^{high}/ESA^{low} cells showed the most potent resistance to cisplatin-induced apoptosis, while CD44^{low} cells had the most marked sensitivity toward induced cell death. The ABC transporter MRP2 (ABCC2) can mediate cisplatin efflux, thus ABCC2 expression has been implicated in cisplatin resistance [13]. We found that ABCC2 mRNA expression was significantly increased in CD44^{high}/ESA^{low} cells among the sorted populations (**Figure 2B**).

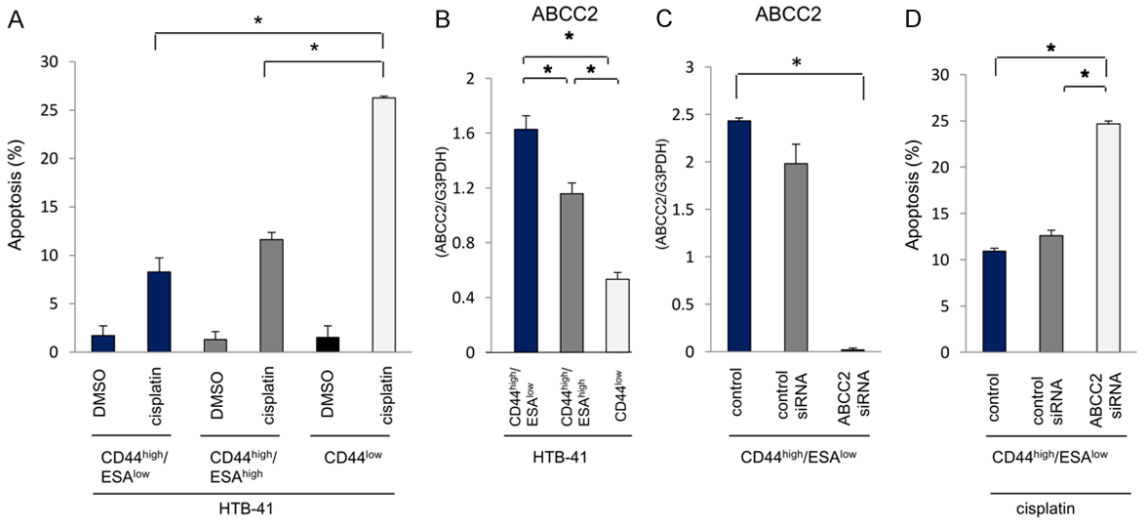

Figure 2. CD44^{high}/ESA^{low} cells exhibit high resistance to cisplatin-induced apoptosis. A. Apoptotic cell death in each of the cell populations was detected by Anexin V staining at 48 hours after cisplatin treatment. The percentage of apoptotic cells was 9.2±1.9%, 13.0±0.77%, and 26.8±0.54% in the CD44^{high}/ESA^{low}, CD44^{high}/ESA^{high}, and CD44^{low} populations, respectively. B. mRNA expression of ABCC2. The CD44^{high}/ESA^{low} cells showed a higher level of ABCC2 mRNA expression as compared with CD44^{high}/ESA^{high} and CD44^{low}. C. siRNA knockdown of ABCC2 in CD44^{high}/ESA^{low} cells. ABCC mRNA expression was significantly inhibited by siRNA knockdown. D. The percentage of cisplatin-induced apoptotic cells in the CD44^{high}/ESA^{low} population was significantly increased by siRNA knockdown of ABCC2. *Statistically significant, as shown by a *P*-value <0.05.

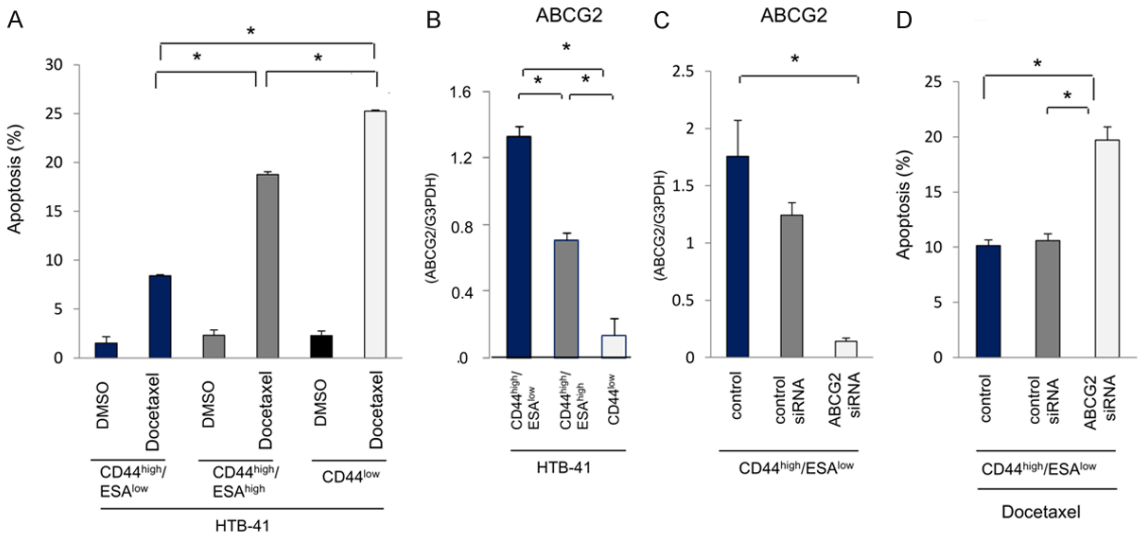

Figure 3. CD44^{high}/ESA^{low} cells exhibit high resistance to docetaxel-induced apopotsis. A. Apoptotic cell death after docetaxel treatment. The percentage of apoptotic cells in the CD44^{high}/ESA^{low}, CD44^{high}/ESA^{high} and CD44^{low} populations was 8.42±0.10%, 18.8±0.32%, and 25.3±0.11%, respectively. B. mRNA expression of ABCG2. CD44^{high}/ESA^{low} cells showed a higher level of ABCG2 mRNA expression as compared to CD44^{high}/ESA^{high} and CD44^{low} cells. C. siRNA knockdown of ABCG2 in CD44^{high}/ESA^{low} cells. ABCG mRNA expression was significantly inhibited by siRNA knockdown. D. The percentage of docetaxel-induced apoptotic cells was significantly increased by siRNA knockdown of ABCG2 in CD44^{high}/ESA^{low} cells. *Statistically significant, as shown by a *P*-value <0.05.

In addition, siRNA knockdown of ABCC2 significantly induced apoptosis of CD44^{high}/ESA^{low} cells in the presence of cisplatin (**Figure 2C**, **2D**). These results suggest that the strong resistance of CD44^{high}/ESA^{low} cells to cisplatin is attributable to a high expression of ABCC2.

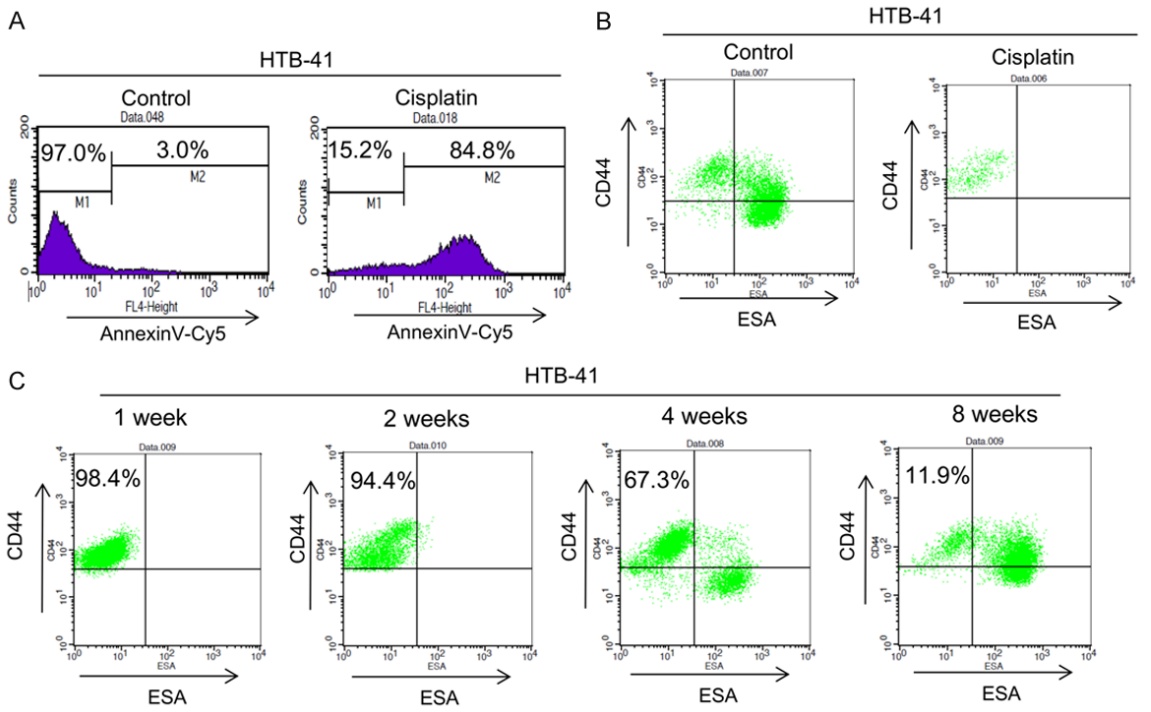

Figure 4. CD44^{high}/ESA^{low} cells reconstitute phenotypic heterogeneity of parent cells. A. At 7 days after cisplatin treatment, 84.8% of HTB-41 cells showed apoptotic cell death in FACS analysis findings. B. FACS analysis of CD44 and ESA in HTB-41 cells that survived after treatment with cisplatin revealed them to be CD44^{high}/ESA^{low} cells. C. Analysis of CD44 and ESA in FACS-sorted CD44^{high}/ESA^{low} cells showed that they reconstituted the phenotypic heterogeneity of the parent cells HTB-41 after 8 weeks.

The percentage of docetaxel-induced apoptotic cells in the CD44^{high}/ESA^{low}, CD44^{high}/ESA^{high}, and CD44^{low} cell populations was 8.42±0.10%, 18.8±0.32%, and 25.3±0.11%, respectively (**Figure 3A**). The CD44^{high}/ESA^{low} group showed the highest level of resistance to docetaxel-induced apoptosis among the groups (**Figure 3A**). Docetaxel is considered to be a substrate for ABCG2 [14]. In the present study, the expression of ABCG2 mRNA was higher in CD44^{high}/ESA^{low} cells as compared to the other phenotypes (**Figure 3B**). In addition, siRNA knockdown of ABCG2 significantly induced apoptosis of CD44^{high}/ESA^{low} cells in the presence of docetaxel (**Figure 3C**, **3D**). These results indicate that CD44^{high}/ESA^{low} cells with a high expression of the ABC transporter gene have potent resistance to cisplatin- and docetaxel-induced apoptosis.

Surviving CD44^{high}/ESA^{low} cells reconstituted the phenotypic heterogeneity of parent cells

After treating HTB-41 parent cells with cisplatin for 7 days, more than 80% were apoptotic, as shown by FACS analysis (**Figure 4A**). Next, CD44 and ESA expressions were examined in the remaining viable HTB-41 cells by FACS, which showed that only CD44^{high}/ESA^{low} cells had survived (**Figure 4B**). The surviving CD44^{high}/ESA^{low} population was sorted by FACS and cultured for up to 8 weeks. After 4 weeks, ESA^{high} cells were observed and the surviving CD44^{high}/ESA^{low} cells completely reconstituted the phenotypic heterogeneity of the parent cells after 8 weeks of culture (**Figure 4C**).

Exogenous PGE_2 induced EMT of CD44^{high}/ESA^{high} cells

Next, we examined the effects of PGE_2 on the sorted populations, as our previous study revealed that PGE_2 was more abundant in SCC tissues as compared to normal tissues and involved in resistance to apoptosis of HNSCC cells [15]. In the present study, we found that 11.2% of the CD44^{high}/ESA^{high} cells were changed into CD44^{high}/ESA^{low} cells after 48 hours of culture in the presence of PGE_2 (**Figure 5A**), whereas neither the CD44^{high}/ESA^{low} nor

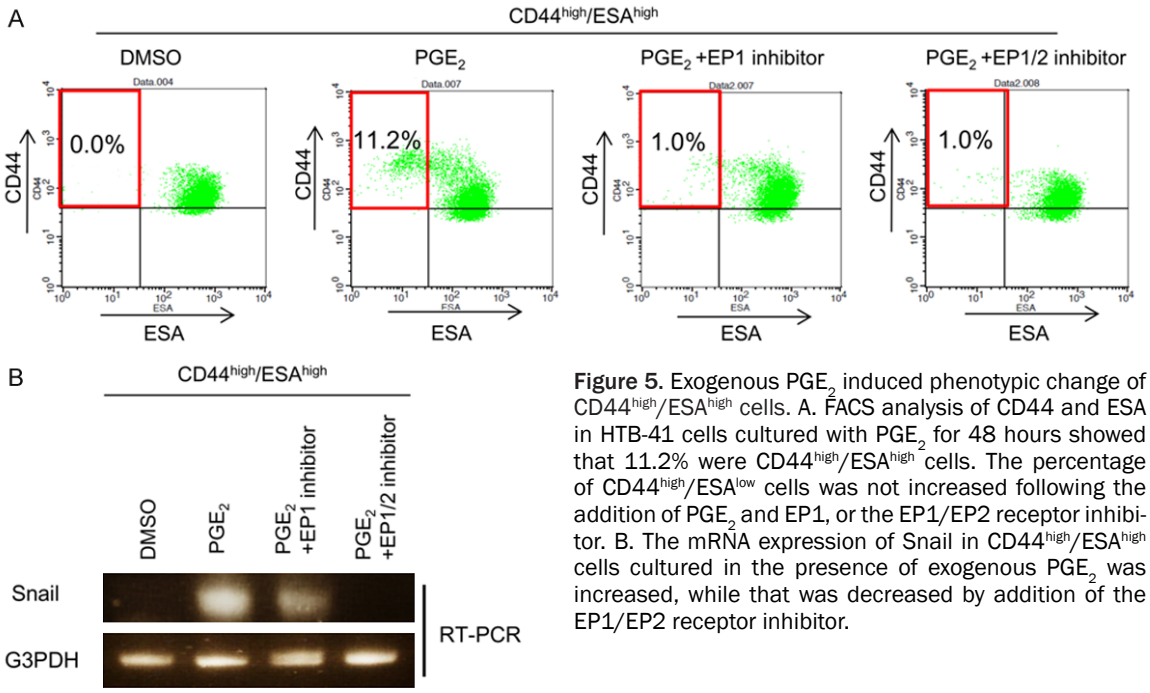

Figure 5. Exogenous PGE_2 induced phenotypic change of CD44^{high}/ESA^{high} cells. A. FACS analysis of CD44 and ESA in HTB-41 cells cultured with PGE_2 for 48 hours showed that 11.2% were CD44^{high}/ESA^{high} cells. The percentage of CD44^{high}/ESA^{low} cells was not increased following the addition of PGE_2 and EP1, or the EP1/EP2 receptor inhibitor. B. The mRNA expression of Snail in CD44^{high}/ESA^{high} cells cultured in the presence of exogenous PGE_2 was increased, while that was decreased by addition of the EP1/EP2 receptor inhibitor.

CD44^{low} cells showed phenotypic change (data not shown). In addition, an inhibitor of the PGE_2 receptors EP1 and EP2 blocked the change into CD44^{high}/ESA^{low} cells by CD44^{high}/ESA^{high} cells (**Figure 5A**), indicating that PGE_2 is involved in the phenotypic change of CD44^{high}/ESA^{high} cells via those receptors. In addition, the mRNA expression of Snail was increased in the presence of PGE_2, whereas PGE_2-induced Snail expression was reduced in the presence of the EP1/EP2 receptor inhibitor (**Figure 5B**). These results suggest that exogenous PGE_2 may enhance EMT of CD44^{high}/ESA^{high} cells by induction of Snail.

Snail-induced CD44^{high}/ESA^{low} cells showed high resistance to cisplatin- and docetaxel-induced apoptosis

Using a pool of OM-1 cells harboring a Snail transgene (OM-1 Snail pool), we previously found that the response of oral SCC cells to Snail is variable [12]. In the present study, we used an OM-1 Snail pool to investigate the population with high CD44 expression. Initially, we examined the expressions of vimentin, ESA, and CD44 in the OM-1 Snail pool. Vimentin mRNA expression was increased and that of ESA was decreased in the OM-1 Snail pool as compared to the control OM-1 cells (**Figure 6A**). Interestingly, CD44 mRNA expression was also apparently increased in the OM-1 Snail pool (**Figure 6A**). Next, we performed FACS analysis of CD44 and ESA expressions in the OM-1 Snail pool. Despite the finding that CD44^{high}/ESA^{low} cells were not detected among the OM-1 control cells, 15.3% of the OM-1 Snail pool was composed of CD44^{high}/ESA^{low} cells (**Figure 6B**). Next, we sorted the CD44^{high}/ESA^{low} population from the OM-1 Snail pool, and examined ABC transporter expression and apoptosis induced by cisplatin. CD44^{high}/ESA^{low} cells from that pool showed high levels of mRNA expressions of ABCC2 and ABCG2 as compared to the OM-1 control cells (**Figure 6C**). The percentage of cisplatin-induced apoptotic cells among CD44^{high}/ESA^{low} cells from the OM-1 snail pool was 8.2±0.85%, while that among the control cells was 28.4±1.1% (**Figure 6D**). In addition, CD44^{high}/ESA^{low} cells from the OM-1 snail pool showed a lower percentage of docetaxel-induced apoptotic cells as compared to the OM-1 control cells (10.6±0.47% vs. 17.9±0.25%) (**Figure 6D**). These results indicate that Snail-induced CD44^{high}/ESA^{low} cells have strong resistance to cisplatin- and docetaxel-induced apoptosis.

Discussion

Although platinum-based chemotherapy has been used for several years to treat head and

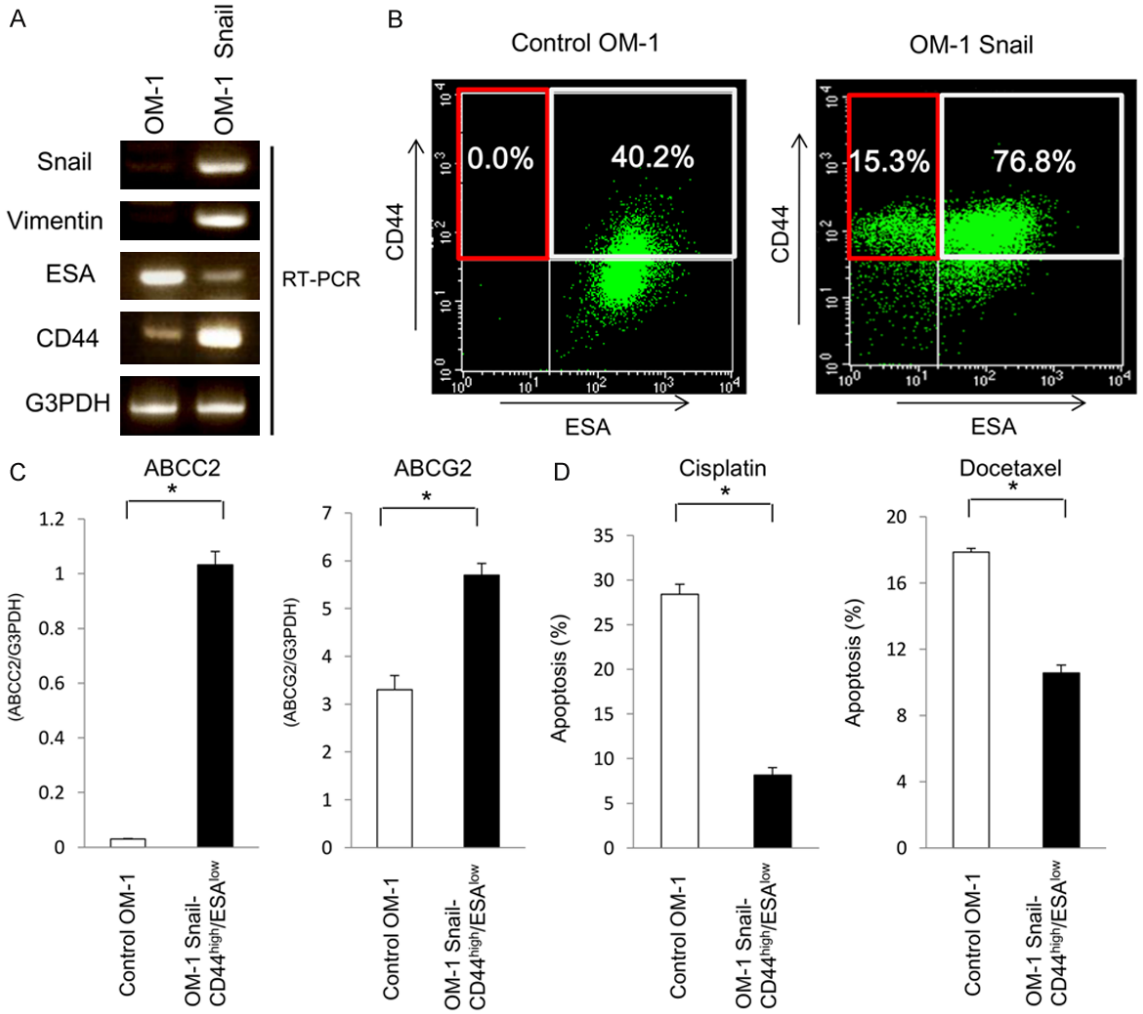

Figure 6. Snail can induce CD44^{high}/ESA^{low} phenotype in OM-1 cells. A. mRNA expressions of vimentin, CD44, and ESA in CD44^{high}/ESA^{low} population from OM-1 Snail pool. The mRNA expressions of vimentin and CD44 were increased, while that of ESA was decreased in those cells as compared to control OM-1 cells. B. FACS analysis of the OM-1 Snail pool for CD44 and ESA showed that 15.3% of those cells were a CD44^{high}/ESA^{low} population. C. CD44^{high}/ESA^{low} cells from the OM-1 Snail pool showed significantly higher expression levels of ABCC2 and ABCG2 mRNA as compared to the OM-1 control. D. Apoptotic cell death after treatment with cisplatin or docetaxel treatment for 48 hours. The percentage of CD44^{high}/ESA^{low} cells from the OM-1 Snail pool and in the OM-1 control showing cisplatin-induced apoptosis was 8.2±0.85% and 28.4±1.1%, respectively, while that of those showing docetaxel-induced apoptosis was 10.6±0.47% and 17.9±0.25%, respectively. *Statistically significant, as shown by a *P*-value <0.05.

neck cancer [16], patients with advanced stage HNSCC show potent resistance to cisplatin, resulting in poor prognosis [17]. The major cytotoxic function of cisplatin is mediated by the development of DNA adducts that can lead to DNA double-strand breakage [18]. Cisplatin resistance may arise from increased efflux ability, decreased uptake, and inhibition caused by intracellular apoptosis-related signaling [19, 20]. On the other hand, taxanes (i.e., docetaxel and paclitaxel) function as anti-cancer drugs by disruption of microtubule assembly, and have been shown to improve the prognosis of HNSCC patients when administered in combination with other chemotherapeutics such as 5-FU and cisplatin [21, 22]. However, alterations of tubulin composition by mutation and post-transcriptional modification of tubulin may be involved in the resistance to taxanes by cancer cells [23]. In the present study, we found that ABC transporter gene expression as well as the percentage of cells with high ABC transporter activity was increased in CD44^{high} as compared to CD44^{low} cells, suggesting that CD44^{high} cells

have an anti-apoptosis characteristic when exposed to chemotherapeutics based on increased drug efflux capacity. In addition, CD44^{high}/ESA^{low} cells showed the most potent resistance to apoptosis induced by cisplatin and docetaxel, while that resistance was blocked by knockdown of the ABC transporter gene. These results indicate that strong resistance to cisplatin and docetaxel may be associated with a high drug efflux capacity of the ABC transporter in CD44^{high}/ESA^{low} cells in HNSCC.

Biddle et al. demonstrated that CD44^{high}/ESA^{low} HNSCC cells had both CSC properties and apparent mesenchymal features [9]. In addition, they showed that those cells have a capability to change their mesenchymal characteristics into epithelial ones and reconstitute the cellular heterogeneity of parent cells, thus demonstrating a tumor forming ability in animal models. Those observations indicate that surviving CD44^{high}/ESA^{low} cells have an ability to invade and undergo mesenchymal to epithelial transition (MET) to produce new tumors at a distant site. Therefore, it has been speculated that the presence of CD44^{high}/ESA^{low} cells is related to worse prognosis (i.e., tumor recurrence and distant metastasis) in patients with HNSCC, because of their tumor initiating capability and high resistance to apoptosis [9, 10].

HNSCC cells are thought to originate from either stem cells of the oral epithelium or through dedifferentiation of cells in the early stage of differentiation, and known to display substantial heterogeneity in regard to phenotypic characteristics (i.e., morphology, growth, and motility) [24, 25]. Accumulated genetic alterations resulting from genomic instability may give rise to such phenotypic heterogeneity of tumor cells [26]. On the other hand, cellular heterogeneity may also arise from epigenetic factors [27]. EMT programs are thought to be important regulators of phenotypic plasticity in embryonic and cancer cells [28], and such epithelial to mesenchymal plasticity has been implicated in the ability of cancer patients to either escape from cancer therapy or have a poor prognosis. Snail, a transcription factor associated with EMT, mainly based on its repression of E-cadherin [29], is required for DeltaNp63 promoter activity and involved in enhancing the invasion ability of oral SCC cells [30]. In addition, this factor can be induced by combined treatment with the cytokines TGFβ, TNFα, and PDGF-D, suggesting that exogenous factors such as cytokines are involved in EMT of HNSCC cells [12]. In this study, we found that exogenous PGE_2 also induced EMT via Snail in oral SCC cells with epithelial characteristics. Importantly, EMT in individual cells of the Snail pool is variable and conditional, even when Snail is constitutively expressed in all cells [12]. These results indicate that Snail plays a vital role in driving partial (i.e., metastable) EMT in HNSCCs [31]. Furthermore, our findings are the first to show that Snail increases the expression of CD44, which is a significant CSC marker of HNSCC. Thus, Snail may be importantly involved in induction of both mesenchymal characteristics and CSC-like properties in HNSCC cells.

In conclusion, CD44^{high}/ESA^{low} HNSCC cells play a central role in resistance to cisplatin and docetaxel based on high drug efflux ability. Furthermore, Snail is importantly involved in induction of CD44^{high}/ESA^{low} cells in HNSCC. To improve the results of chemotherapy for HNSCC patients, a better understanding of the phenotypic plasticity of CD44^{high} cells may be required. To advance current therapeutic approaches, it is considered necessary to target CD44^{high} cells with mesenchymal characteristics in order to overcome resistance to apoptosis induced by cisplatin and docetaxel.

Acknowledgements

This study was supported by a Grant-in-aid for Scientific Research (C) (No. 26463005) from the Japanese Ministry of Education, Culture, Sports, and Technology. A portion of this work was carried out at the Analysis Center of Life Science, Natural Science Center for Basic Research and Development, Hiroshima University. We thank Dr. Hayashi and Dr. Harada for their technical assistance with the FACS sorting.

Disclosure of conflict of interest

None.

Address correspondence to: Hideo Shigeishi, Department of Oral and Maxillofacial Surgery, Division of Cervico-Gnathostomatology, Graduate School of Biomedical Sciences, Hiroshima University, 1-2-3 Kasumi, Minami-ku, Hiroshima 734-8553, Japan. Tel: +81-82-257-5673; Fax: +81-82-257-5671; E-mail: shige@hiroshima-u.ac.jp

References

[1] Warnakulasuriya S. Global epidemiology of oral and oropharyngeal cancer. Oral Oncol 2009; 45: 309-316.

[2] Petersen PE. Oral cancer prevention and control-the approach of the World Health Organization. Oral Oncol 2009; 45: 454-460.

[3] Bernier J, Domenge C, Ozsahin M, Matuszewska K, Lefèbvre JL, Greiner RH, Giralt J, Maingon P, Rolland F, Bolla M, Cognetti F, Bourhis J, Kirkpatrick A and van Glabbeke M. Postoperative irradiation with or without concomitant chemotherapy for locally advanced head and neck cancer. N Engl J Med 2004; 350: 1945-1952.

[4] Vermorken JB, Mesia R, Rivera F, Remenar E, Kawecki A, Rottey S, Erfan J, Zabolotnyy D, Kienzer HR, Cupissol D, Peyrade F, Benasso M, Vynnychenko I, De Raucourt D, Bokemeyer C, Schueler A, Amellal N and Hitt R. Platinum-based chemotherapy plus cetuximab in head and neck cancer. N Engl J Med 2008; 359: 1116-1127.

[5] Forastiere AA. Overview of platinum chemotherapy in head and neck cancer. Semin Oncol 1994; 21: 20-27.

[6] Prince ME, Sivanandan R, Kaczorowski A, Wolf GT, Kaplan MJ, Dalerba P, Weissman IL, Clarke MF and Ailles LE. Identification of a subpopulation of cells with cancer stem cell properties in head and neck squamous cell carcinoma. Proc Natl Acad Sci U S A 2007; 104: 973-978.

[7] Chikamatsu K, Ishii H, Takahashi G, Okamoto A, Moriyama M, Sakakura K and Masuyama K. Resistance to apoptosis-inducing stimuli in CD44+ head and neck squamous cell carcinoma cells. Head Neck 2012; 34: 336-343.

[8] Prince ME, Sivanandan R, Kaczorowski, Wolf GT, Kaplan MJ, Dalerba P, Weissman IL, Clarke MF and Ailles LE. Identification of a subpopulation of cells with cancer stem cell properties in head and neck squamous cell carcinoma. Proc Natl Acad Sci U S A 2007; 104: 973-978.

[9] Biddle A, Liang X, Gammon L, Fazil B, Harper LJ, Emich H, Costea DE and Mackenzie IC. Cancer stem cells in squamous cell carcinoma switch between two distinct phenotypes that are preferentially migratory or proliferative. Cancer Res 2011; 71: 5317-5326.

[10] Shigeishi H, Biddle A, Gammon L, Rodini CO, Yamasaki M, Seino S, Sugiyama M, Takechi M and Mackenzie IC. Elevation in 5-FU-induced apoptosis in head and neck cancer stem cells by a combination of CDHP and GSK3β inhibitors. J Oral Pathol Med 2015; 44: 201-207.

[11] Taki M, Kamata N, Yokoyama K, Fujimoto R, Tsutsumi S and Nagayama M. Down-regulation of Wnt-4 and up-regulation of Wnt-5a expression by epithelial-mesenchymal transition in human squamous carcinoma cells. Cancer Sci 2003; 94: 593-597.

[12] Okui G, Tobiume K, Rizqiawan A, Yamamoto K, Shigeishi H, Ono S, Higashikawa K and Kamata N. AKT primes snail-induced EMT concomitantly with the collective migration of squamous cell carcinoma cells. J Cell Biochem 2013; 114: 2039-2049.

[13] Kool M, de Haas M, Scheffer GL, Scheper RJ, van Eijk MJ, Juijn JA, Baas F and Borst P. Analysis of expression of cMOAT (MRP2), MRP3, MRP4, and MRP5, homologues of the multidrug resistance-associated protein gene (MRP1), in human cancer cell lines. Cancer Res 1997; 57: 3537-3547.

[14] Xie Y, Xu K, Linn DE, Yang X, Guo Z, Shimelis H, Nakanishi T, Ross DD, Chen H, Fazli L, Gleave ME and Qiu Y. The 44-kDa Pim-1 kinase phosphorylates BCRP/ABCG2 and thereby promotes its multimerization and drug-resistant activity in human prostate cancer cells. J Biol Chem 2008; 283: 3349-3356.

[15] Shigeishi H, Higashikawa K, Hatano H, Okui G, Tanaka F, Tran TT, Rizqiawan A, Ono S, Tobiume K and Kamata N. PGE_2 targets squamous cell carcinoma cell with the activated epidermal growth factor receptor family for survival against 5-fluorouracil through NR4A2 induction. Cancer Lett 2011; 307: 227-236.

[16] Kalavrezos N and Bhandari R. Current trends and future perspectives in the surgical management of oral cancer. Oral Oncol 2010; 46: 429-432.

[17] Jacobs C, Lyman G, Velez-García E, Sridhar KS, Knight W, Hochster H, Goodnough LT, Mortimer JE, Einhorn LH and Schacter L. A phase III randomized study comparing cisplatin and fluorouracil as single agents and in combination for advanced squamous cell carcinoma of the head and neck. J Clin Oncol 1992; 10: 257-263.

[18] Chu G. Cellularresponses to cisplatin. The roles of DNA-binding proteins and DNA repair. J Biol Chem 1994; 269: 787-790.

[19] Siddik ZH. Cisplatin: mode of cytotoxic action and molecular basis of resistance. Oncogene 2003; 47: 7265-7279.

[20] Galluzzi L, Senovilla L, Vitale I, MichelsJ, Martins I, Kepp O, Castedo M and Kroemer G. Molecular mechanisms of cisplatin resistance. Oncogene 2012; 31: 1869-1883.

[21] Sparano JA. Taxanes for breast cancer: an evidence-based review of randomized phase II and phase III trials. Clin Breast Cancer 2000; 1: 32-40.

[22] Yang WC, Chen CH, Tang JY, Wu CF, Liu YC, Sun Y and Lin SF. Induction chemotherapy with docetaxel, cisplatin and fluorouracil followed

by surgery and concurrent chemoradio therapy improves outcome of recurrent advanced head and neck squamous cell carcinoma. Anticancer Res 2014; 34: 3765-3773.

[23] Orr GA, Verdier-Pinard P, McDaid H and Horwitz SB. Mechanisms of Taxol resistance related to microtubules. Oncogene 2003; 22: 7280-7295.

[24] Tang XH, Scognamiglio T and Gudas LJ. Basal stem cells contribute to squamous cell carcinomas in the oral cavity. Carcinogenesis 2013; 34: 1158-1164.

[25] Vig N, Mackenzie IC and Biddle A. Phenotypicplasticity and epithelial-to-mesenchymal transition in the behaviour and therapeutic response of oral squamous cell carcinoma. J Oral Pathol Med 2015; 44: 649-655.

[26] Ashworth A, Lord CJ and Reis-Filho JS. Genetic interactions in cancer progression and treatment. Cell 2011; 145: 30-38.

[27] Marusyk A, Almendro V and Polyak K. Intra-tumour heterogeneity: a looking glass for cancer? Nat Rev Cancer 2012; 12: 323-334.

[28] Tam WL and Weinberg RA. The epigenetics of epithelial-mesenchymal plasticity in cancer. Nat Med 2013; 19: 1438-1449.

[29] Kalluri R and Weinberg RA. The basics of epithelial-mesenchymal transition. J Clin Invest 2009; 119: 1420-1428.

[30] Higashikawa K, Yoneda S, Tobiume K, Taki M, Shigeishi H and Kamata N. Snail-induced down-regulation of DeltaNp63 alpha acquires invasive phenotype of human squamous cell carcinoma. Cancer Res 2007; 67: 9207-9213.

[31] Tam WL and Weinberg RA. The epigenetics of epithelial-mesenchymal plasticity in cancer. Nat Med 2013; 19: 1438-1449.